Smart Structures and Systems, Vol. 8, No. 2 (2011) 219-237
DOI: http://dx.doi.org/10.12989/sss.2011.8.2.219

Identification of multiple sources in a plate structure using pre-filtering process for reduction of interference wave

S.K. Lee*, Y.S. Moon and J.H. Park

Department of Mechanical Engineering, Inha University, 253 Yonghyun-Dong,Nam-Gu, Incheon 402-751, Korea

(Received December 8, 2010, Accepted May 24, 2011)

Abstract. This paper presents novel research into the source localization of multiple impacts. Source localization technology for single impact loads in a plate structure has been used for health monitoring. Most of research on source localization has been focused only on the localization of single impacts. Overlapping of dispersive waves induced by multiple impacts and reflection of those waves from the edge of the plate make it difficult to localize the sources of multiple impacts using traditional source localization technology. The method solving the overlapping problem and the reflection problem is presented in the paper. The suggested method is based on pre-signal processing technology using band pass filter and optimal filter. Results from numerical simulation and from experimentation are presented, and these verify the capability of the proposed method.

Keywords: plate; piezoelectronic sensor; multiple sources localization; reflection; optimal filter.

1. Introduction

The localization of impact sources is applied to the identification of impact damage (Ziola and Gorman 1991, Loutridis *et al.* 2005, Raghavan and Cesnik 2007), to loose part monitoring in nuclear power plants (Park and Kim 2006, Lee and Kim 2008), to crack analysis in non-destructive evaluation (Balasubramaniam and Rose 1991, Prosser *et al.* 1999), and to human-interaction technology in electronic devices (Pham *et al.* 2007, Rolshofen *et al*. 2007), etc. Thus far, mostly single-impact source localization technology (SLT) has been used in those applications. SLT for a single impact on a plate is mostly based on the estimation of arrival time of the elastic wave from the impact location to three sensors, which are attached to the plate. These arrival times are obtained from time frequency analysis (TFA) for the elastic wave generated by the impact load on the plate. The elastic wave detected by the three sensors has dispersive characteristics, and TFA is a useful signal processing tool for the analysis of a dispersive wave (Ziola and Gorman 1991, Raghavan and Cesnik 2007, Park and Lee 2010). Wigner distribution is used for single impact localization (Park and Kim 2006). High order Wigner distribution is used for single impact localization (Lee *et al.* 2007) and is applied to the nuclear power plant (Lee and Kim 2008). However, when multiple impacts are loaded on the plate, it is difficult to localize the sources of multiple impacts by using the current SLT because of the overlapping of the elastic waves and the reflection of those waves from the edge in a plate (Loutridis *et al.* 2005). In this paper, a new

*Corresponding Author, Professor, E-mail: sangkwon@inha.ac.kr

method is suggested for the source localization of multiple impacts. The proposed method uses pre-processed signal processing to solve the overlapping and reflection problems. The pre-processed signal processing is developed by using a band pass filter and a linear-prediction filter. This pre-processed signal processing is applied to the elastic wave measured by the sensors installed on the plate. The pre-processed waveforms are analyzed by the TFA method to obtain the arrival time. At the sensors, the arrival time differences of the wave front are used for the estimation of impact source using triangulation. In the second section, SLT for single impacts is explained to identify the problem that should be considered for the source localization of multiple impacts in a plate. In the third section, the problems of and solutions for the source localization of multiple impacts are demonstrated. The fourth section presents the procedure for the source localization of multiple impacts and its application in a plate. Conclusions are given in the section five.

2. Source localization of a single impact in a plate

2.1 Plate theory

The theoretical solution to the response of a plate subject to surface or subsurface impact sources is a topic of considerable current research interest. The solution of three-dimensional problems involving homogeneous or multilayered isotropic and anisotropic plates of finite thickness and large lateral dimensions subjected to various types of surface loads has been given earlier in Ref (Lih and Mal 1995) and will not be repeated here. For a homogeneous, isotropic plate of infinite dimensions in the x_1 and x_2 directions (Fig. 1), the elastodynamic field can be conveniently expressed in terms of a six dimensional, stress-displacement vector $\{\hat{S}\}$ in the frequency domain, as

$$\{\hat{S}(k_1, k_2, x_3, \omega)\} = \{\hat{u}_i \ \hat{\sigma}_{i3}\}, i = 1, 2, 3 \tag{1}$$

where, $\hat{u}_i$ and $\hat{\sigma}_i$ are the displacement and stress components, k_1 and k_2 are the wavenumbers in directions 1 and 2, and ω is the circular frequency. The stress-displacement vector can be obtained in the frequency domain through the solution of a system of first order equations supplemented by appropriate boundary conditions, resulting in a system of linear equations of order 6. The boundary conditions on the faces of the plate are

$$\hat{\sigma}_{i3}^1(x_1, x_2, 0, \omega) = -\hat{F}_i(x_1, x_2, \omega) \tag{2a}$$

$$\hat{\sigma}_{i3}^1(x_1, x_2, H, \omega) = 0 \tag{2b}$$

where $\hat{F}_i$ is the Fourier time transform of the spatially distributed impact load. In general, the surface displacement can be expressed in the wavenumber integral form

$$I = \frac{1}{4\pi^2}\int_{-\infty}^{\infty}\int_{-\infty}^{\infty}\frac{f(k_1, k_2, \omega)}{g(k_1, k_2, \omega)}e^{i(k_1x_1 + k_2x_2)}dk_1dk_2 \tag{3}$$

where I is the 3D surface displacement. The functions f and g are obtained by solving the system of linear equations as indicated earlier. This integral must be evaluated numerically for a large number of frequency points, and the resulting spectra can then be inverted by FFT to determine the time dependent displacement and stress components.

2.2 Numerical results

A major objective of this section is to determine the impact location throughout the measurement of the acoustic signal at the arbitrary point *r* in the plate, as shown in Fig. 1. The plate used for this numerical analysis is isotropic aluminum plate. The phase velocity of this plate can be calculated with exact plate theory (Alleyne and Cawley 1991), Mindlin's approximate shear deformation plate theory (SDPT) (Mindlin 1951), and classic plate theory (CPT) (Graff 1953). An important wave mode in the impact testing of structures is the Lamb wave. This wave mode is named after Horace Lamb, an English acoustician who in the 1920s developed the mathematical theory of sine waves propagating in finite plates (Hellier 2003). This kind of theory seeks to describe wave propagation in terms of wave modes-patterns of oscillatory motion that can propagate in a stable way, maintaining their shape as they travel. In plates, Lamb identified two families of wave modes, and he developed equations that described their velocities of propagation. In the first family, the motion is symmetrical about the median plane of the plate, and in the second family it is asymmetrical. The parent members of these families are called the s_0 and a_0 modes, respectively. The s_0 mode, often called the "extensional mode," is a rippling movement in which the plate is alternately stretching and compressing in the direction of the wave motion. Coupled with this in-plane movement, the sides of the plate are "breathing" in and out symmetrically as the ripples run through the plate. To produce this kind of wave motion, the exciting force needs to be directed parallel to the plate. A sudden release of in-plane tension will also tend to produce this kind of wave motion. The a_0 mode, often called the "flexural mode," is a mode in which the body of the plate bends with the two surfaces moving in the same direction. Most of the motion is transverse to the plate; there is relatively little motion in the plane of the plate. Exciting forces perpendicular to the plate produce this kind of wave motion. In addition to this, forces that are parallel to the plate but offset from the center line can produce this wave mode. Fig. 2 shows dispersive curves for the multi mode of an aluminum plate with dimensions 1200 mm × 1200 mm and 10 mm. According to the dispersive curves shown in Fig. 2, up to 0.1 MHz, the a_0 antisymmetric flexible mode and s_0 symmetric modes overrule the wave propagation in the plate. The phase velocities of multi modes are obtained by using the SDPT, since the aluminum plate used in this test is thick.

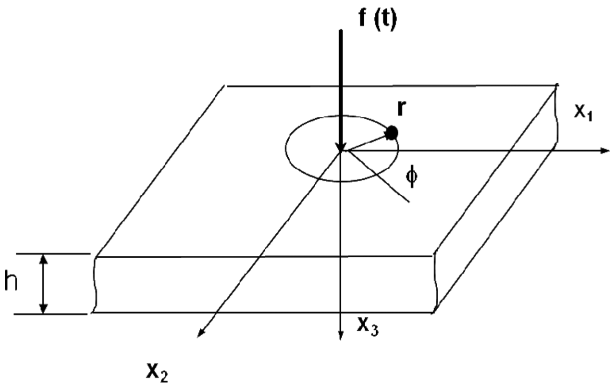

Fig. 1 Geometry of the concentrated load problem

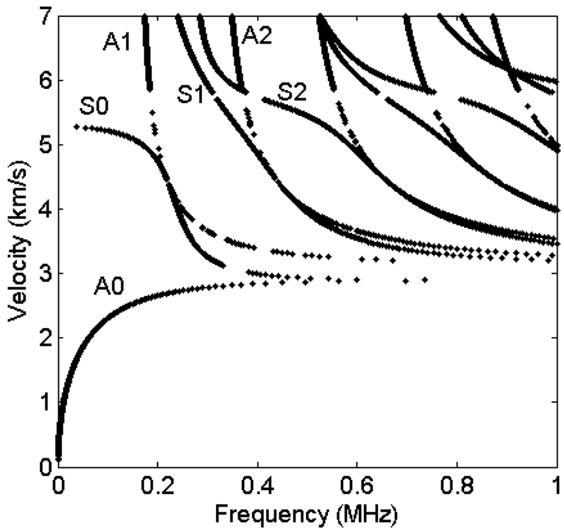

Fig. 2 Dispersive curve for the multi mode of aluminum plate

2.3 Source location technology based on TFA

For the source localization of a single impact, the response to impact load is simulated numerically. The delta function $\delta(t)$ is used for the impact load in a plate, as shown in Fig. 3(a). The displacements at positions S_1, S_2 and S_3 are numerically simulated by using Eq. (3). The location of the impact source can be obtained through triangulation (see Appendix A) using the difference of the traveling times of the waves from the source to the three sensors (Lee *et al.* 2007). It is difficult to measure the arrival time difference of dispersive waves using traditional methods such as the correlation method (Ziola and Gorman 1991), which is useful for non-dispersive waves. The time-frequency method is an effective method for determination of the arrival time of dispersive Lamb waves

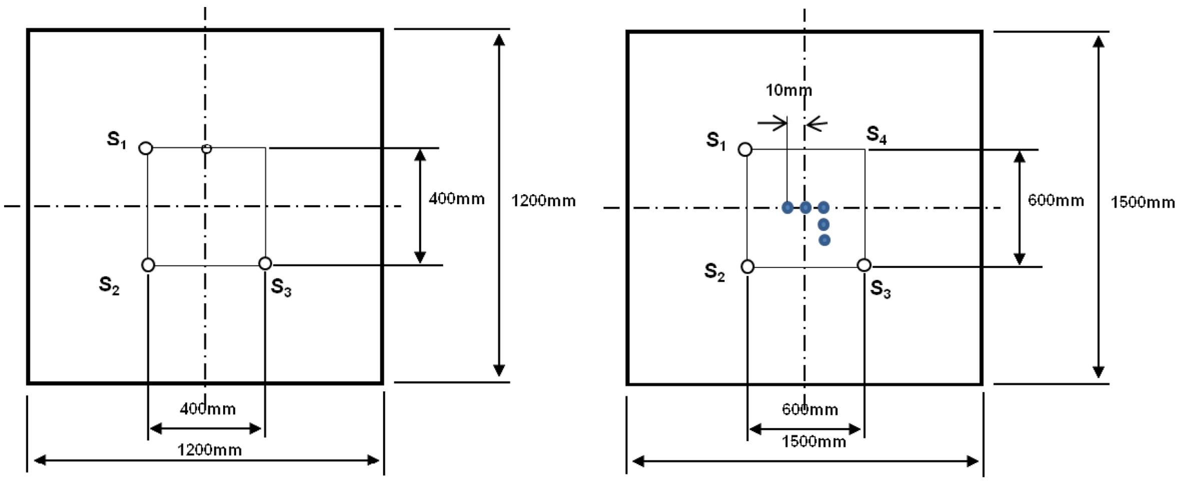

(a) (b)

Fig. 3 Locations of impact load (a) a single impact on an aluminum plate and (b) multiple impacts on a steel plate

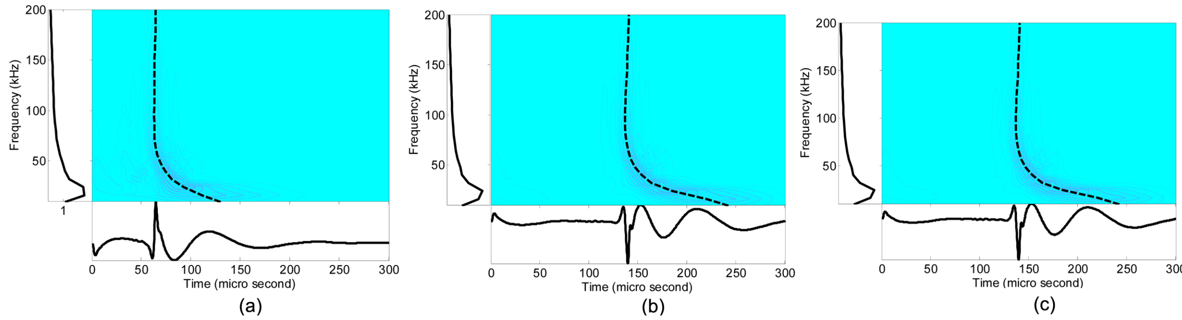

Fig. 4 SWFOMS for the waveforms simulated by the approximated SDPT: (a) Sensor S_1, (b) Sensor S_2 and (c) Sensor S_3

propagating across a plate in an impact test (Loutridis *et al.* 2005, Raghavan and Cesnik 2007, Park and Kim 2006, Lee and Kim 2008). In the present paper, as the time-frequency method, the sliced Wigner fourth-order moment spectrum (SWFOMS) is employed (see Appendix B). The SWFOMS has high time and frequency resolution, compared to other time-frequency methods. The generalized versions of the SWFOMS are given by (Lee 1998)

$$SWFOMS(t, f) = \frac{1}{2}\int_{\tau} \gamma(\tau) W_{2,sw}(f, t+\tau) \cdot W^{*}_{2,sw}(f, t-\tau) d\tau \tag{4}$$

where $W_{2,sw}(t, f)$ is any bilinear distribution (Cohen 1995) and $\gamma(t)$ is a windowing function. The SWFOMS is applied to the simulated waveforms, which are the displacements at positions S_1, S_2 and S_3. The contour map and image analysis for results of the SWFOMS for the displacement waveform are presented in the time-frequency space as shown in Fig. 4. In the figures, the horizontal axis presents time and the vertical axis presents frequency. The dashed lines in the center part of each map correspond to the peak amplitude. The arrival time difference for the waveform is obtained from three dashed lines. The theoretical group velocity is defined as the derivative of the angular frequency with respect to the wave number (Graff 1953). The theoretical group velocity for the simulated wave form is

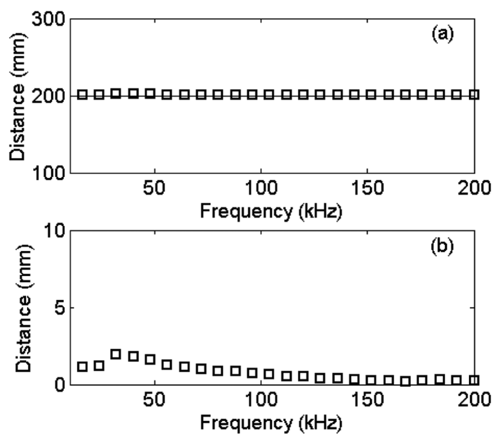

Fig. 5 Estimation of source location and distance error using the group velocity for the waveform simulated by SDPT: (a) Distance from true source and (b) Error in distance estimate

calculated. For this calculation, only the A_0 mode is used. The group velocity of the simulated waveform can be also estimated by dividing the distance between the sensor and the impact source by the arrival time. The location of the impact load is estimated by triangulation (see Appendix A), using the theoretical group velocity and the estimated arrival time difference. This is the current source localization technology (SLT) for source localization of a single impact. Fig. 5 shows the source location of a single impact load estimated by this SLT. Fig. 5(a) shows the estimated location of the source and Fig. 5(b) shows the distance error between the true location and the estimated location. According to these results, the estimation of the location of a single impact load using the current SLT is effective since the distance errors are within 1%.

3. Source localization of multiple impacts in a plate

In the previous section, the source location for a single impact load in a plate is identified successfully by using the current SLT based on time frequency analysis (TFA) for a Lamb wave with dispersive characteristics. However, it is difficult to localize the sources of serial multiple impacts by using the current SLT because of the overlapping of the serial impact waveforms and the reflection of those waves from the edge of a plate. In fact, research on the source localization of multiple impacts based on time frequency analysis (TFA) for Lamb wave has not previously been presented in a research paper. In this section, a novel method for the source localization of serial multiple impacts is proposed by solving the overlapping problem and the reflection problem.

3.1 The overlapping problem and a solution for serial impact waves

When serial five impact loads excite the surface of a plate, as shown in Fig. 3(b), the waveform gen erated by the second impact load is interfered with by the waveform generated by the first impact. The third and fourth waveforms are also interfered with by waveforms from previous impacts, as shown in Fig. 6. In Fig. 6, the symbol Δ is the time interval of multiple impacts. The measured signal for a sensor is the sum of four impact waves and has overlapping problems that prevent the localization of impact sources when using the current SLT based on TFA. Thus, the time history of the signal measured for one sensor is very complex. This problem of overlapping

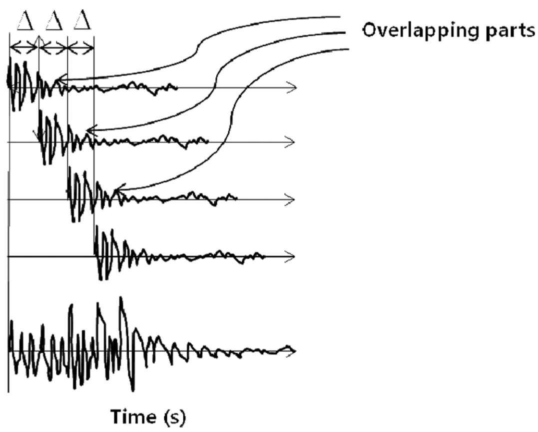

Fig. 6 Impact waveform measured by one sensor attached on the plate

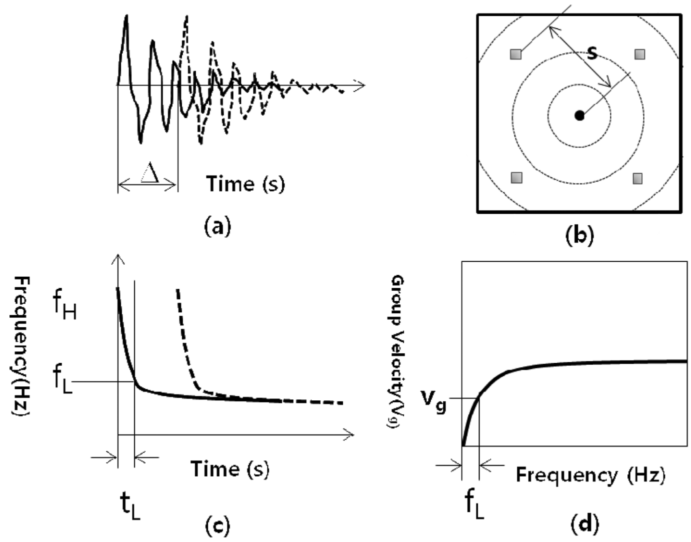

Fig. 7 Pictorial explanation of overlapping of dispersive waves in a plate and of the condition necessary to prevent such overlapping

waveforms from multiple impacts is caused by the dispersive characteristics of waves. Since, at a low frequency, the group velocity of the waves is small, the wave having a low frequency component arrives at the sensor late. This slow wave is overlapped by the wave generated by the next impact. Fig. 7(a) illustrates the overlapping phenomenon. To avoid this overlapping problem at low frequencies, it is necessary to employ a band pass filter. When an impact wave is propagated to the sensor, the distance between the point of impact and the sensor is S, as shown in Fig. 7(b). For example, if two serial impacts excite the plate, the arrival time difference of the two waves is obtained by TFA. The result of the TFA for two waves measured at the sensor is presented in Fig. 7(c). Two dispersive wave signals overlap at a frequency less than the low frequency f_L. Therefore, if the low frequency limit of the high pass filter is selected at this frequency f_L, then the low frequency overlapping can be avoided because the group velocity v_g of the wave above this frequency is fast, as shown in Fig. 7(d), and the wave arrives at the sensor within time t_L. For the simulated wave generated by a single impact in an infinite aluminum plate, the time t_L is around 0.15 milliseconds, as shown in Fig. 4. Therefore, the time interval Δ between serial impacts should be longer than the time t_L. The one condition necessary to prevent overlapping is that the impact interval Δ should be longer than time t_L, and the mathematical expression of this condition is given by

$$\Delta \geq \frac{S}{v_g|_{f_L}} \approx t_L \tag{5}$$

where S is the distance between the impact source and the sensor, and $v_g|_{f_L}$ is the group velocity at low frequency f_L. The high frequency limit for the high pass filtering is the sampling frequency of data. However, if an accelerometer is used as the detection sensor, the resonance frequency of the accelerometer becomes the high frequency limit f_H. Therefore, in this application, a displacement sensor that uses piezo-electric material is useful. Fig. 8 shows a displacement sensor designed with piezo-electronic materials for this research.

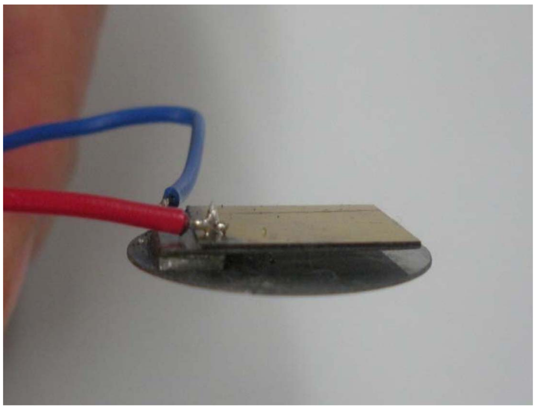

Fig. 8 Piezo-electronic displacement sensor used for this research

3.2 Reflection problem and solution

A wave generated by an impact load is propagated through the sensors attached on the finite plate to the edge of the plate and then reflects from the edge. Therefore, the sensors detect the direct wave and the reflective wave. Since the reflective wave is also dispersive, it has a high group velocity at high frequency and affects the direct wave generated by the next impact. Fortunately, the magnitude of the reflective wave is smaller than that of the direct wave generated by the next impact load since it travels along the plate for a relatively long time and is damped by the structure of the plate (Hellier 2003). However, since the magnitude of the end segment of the direct wave is not sufficiently large, by comparison with the magnitude of the reflective wave, as shown in Fig. 9

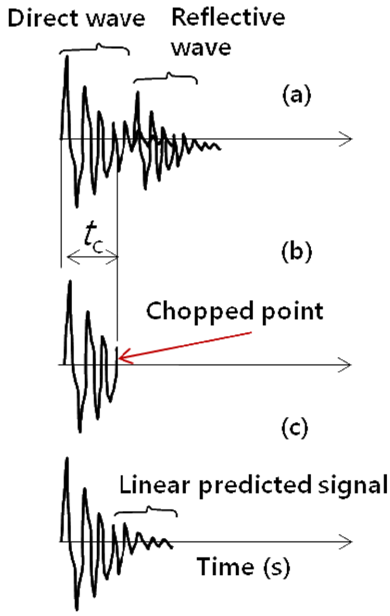

Fig. 9 Illustration of the smoothing process to smooth the high frequency component at the chopped segment of the wave induced by an impact source using the linear prediction filter

(a), it is difficult to discern the reflective wave from the direct wave at the end segment of the direct wave. In order to avoid the effect of the reflective wave at the end segement of the direct wave, only the direct wave should be chopped at this end segment. The time t_c for chopping is determined by using the information obtained from the simulated waveform for the infinite plate, as shown in Fig. 4. For the simulated waveform, the time length of the waveform with wave energy is around 0.15 milliseconds. Fig. 9(b) shows the chopped signal with only the direct wave. In this process, some of the direct wave has the high frequency component due to the chopping at the end of the chopped signal. This high frequency component causes some difficulty in analyzing the dispersive wave in the time frequency domain. Therefore, it is necessary to smooth the chopped signal in order to predict the direct wave continuously at the end segment of the chopped wave. To smooth the chopped wave, a linear-prediction filter is employed (Haykin 2007). The optimal linear-prediction filter is designed by using the Wiener-Horf equation (see Appendix C) and is given by

$$\boldsymbol{f} = \boldsymbol{R}^{-1}\boldsymbol{g} \tag{6}$$

where $\boldsymbol{f}$ is the linear-prediction filter vector, $\boldsymbol{R}$ is the auto correlation matrix vector for input data, $\mathbf{g}$ is the cross correlation vector between the tap input vector, $\boldsymbol{x}(n\text{-}1)$ with M by 1 size and target signal $x(n)$. The target signal $x(n)$ is the desired value that should be predicted using the previous input vector $\boldsymbol{x}(n\text{-}1)$. Fig. 9(c) shows the direct wave containing the signal predicted by the optimal linear-prediction filter.

4. Procedure and application

4.1 Procedure for source localization of multiple impacts

In the previous section, the deadlocks for source location of multiple impacts in a plate are discussed. Novel solutions for those problems were also proposed in section 3. This section presents the procedure for the source localization of multiple impacts with the pre-signal processing method developed in the previous section, and this procedure is applied to source localization in a steel plate. There are two major problems in the source localization of multiple impacts in a plate. One is the overlapping between waveforms generated by multiple impacts, and the other is the reflection at the edge of a plate. Fig. 10 shows a flow chart of the procedure for the source localization of multiple impacts by solving these two problems. First, the displacement of the waveform should be measured. The waveform is affected by both the overlapping and the reflection problems. A band pass filter should be employed to prevent the overlapping problem at low frequencies. The band pass filtered signal still has the reflection problem at high frequencies. In order to avoid the reflection problem, only the direct wave should be chopped at the interface region between the direct wave and the reflective wave. The chopped signal includes high frequency components which should be smoothed to get an exact arrival difference in the time frequency domain by using the time-frequency method. The optimal linear-prediction filter is designed by using the chopped direct wave signal. In order to obtain the arrival time difference at each sensor, the time-frequency method should be applied to the pre-processed waveform throughout the band pass filter and the linear-prediction filter. As a next step, the theoretical group velocity should be calculated by using the Lamb wave theory in a plate and the material properties of the plate. By using this group velocity and the arrival time difference, the sources of multiple impacts can be localized based on triangulation.

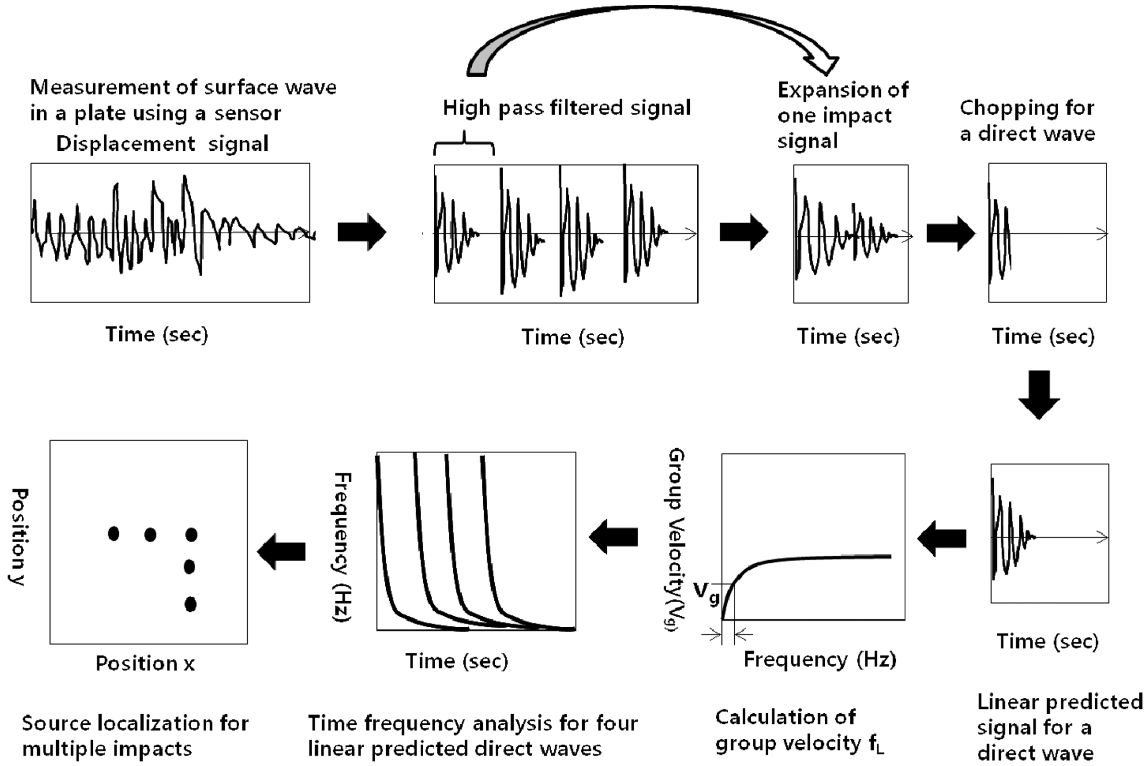

Fig. 10 Flow chart of the procedure for source localization of multiple impacts by solving these two problems in a plate

4.2 Application in an isotropic steel plate

Application of the proposed technology to an isotropic steel plate for the source localization of multiple impacts is described in this section. The steel plate was attached to a firm structure, as shown in Fig. 11. Five impact loads were applied serially to the points marked on the plate. The waves generated by the five impacts propagated to the four attached piezo-electronic displacement sensors, which detected the direct and the reflective waves. Impact tests were carried out on a plate 6 mm in thickness with lateral dimensions of 1500 mm × 1500 mm. Impact load was generated by an instrumented impact pencil. Fig. 12 shows the time history measured by four sensors attached to the plate. The sampling frequency was 50 kHz and the cut-off frequency was 25 kHz. Four impact loads were applied to the plate, and the impact phenomena were not clear in the measured signal because of overlapping and reflection. Fig. 13(a) shows the spectrogram for the raw signal measured at the one of the sensors. In order to prevent the overlapping problem, the band pass filter with a low frequency limit of 10 kHz and a high frequency limit of 20 kHz was applied to the measured signals. Fig. 13(b) shows the spectrogram for the signal filtered using the band pass filter. According to these results, the heavy overlapping problem was solved by applying the band pass filter to the raw signal. Fig. 13(b) shows the clear impact waveform. Next, the reflection wave should also be removed. In order to observe the reflection phenomena, for example, the signal generated by the fourth impact was cut and the cut signal was plotted as shown in Fig. 14. There

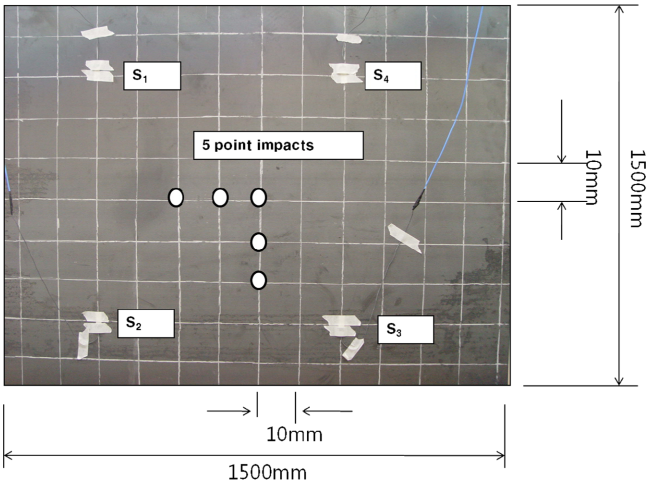

Fig. 11 Photography of impact test for source localization of multiple impacts

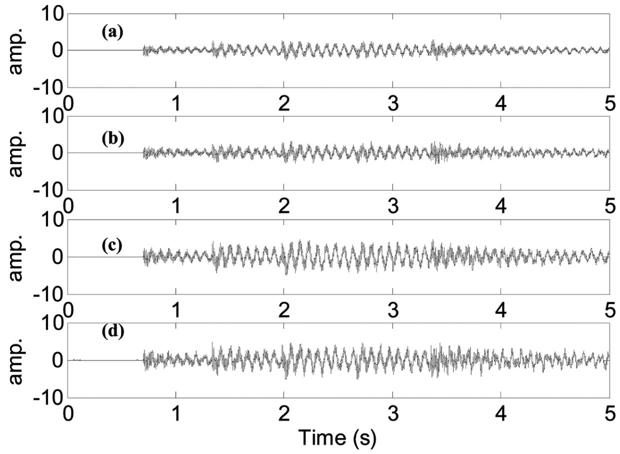

Fig. 12 Time history for the measured waveform through four sensors attached to the plate

are two or three impulsive waves that can be seen in these signals. The first impulsive wave is the direct wave due to the fourth impact and the second impulsive wave or the third impulsive wave is the reflective wave at the edge of the plate. In order to remove the reflective wave from these signals, except for the first impulsive wave of the four signals, the other impulsive waves of the signals was chopped. The chopping time t_c can be determined using the waveform which is obtained by the numerical analysis for the infinite plate, as shown in Fig. 4. For the steel plate, the chopping time t_c was specified as 0.15 milliseconds. The chopped waveforms have the high frequency component at the end. This high frequency component hinders the successful application of time-frequency analysis to get the arrival time difference. In order to smooth the high frequency component, the optimal linear-prediction filter was designed and applied to the chopped signal. The number of tap size M in the linear-prediction filter is 10. The smoothing of the direct waves due to the other impacts was obtained in the same fashion as that of the direct wave due to the fourth impact. The time-

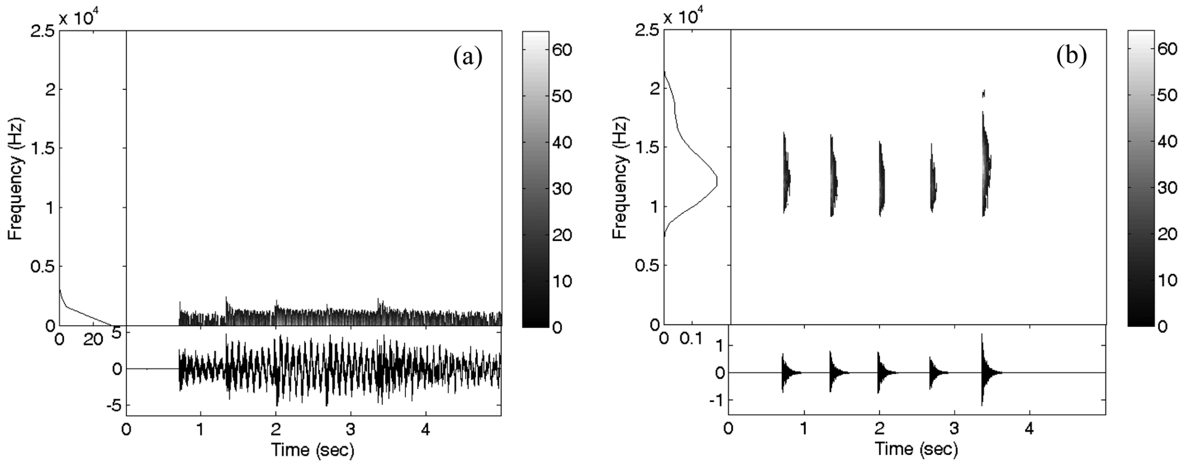

Fig. 13 Spectrogram for one measured waveform: (a) raw signal and (b) high pass filtered signal

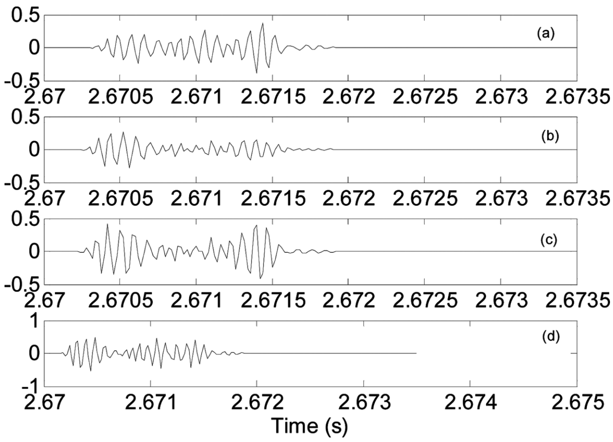

Fig. 14 Time histories of the signals measured by four sensors after the fourth impact: (a) sensor S_1, (b) sensor S_2, (c) sensor S_3 and (d) sensor S_4

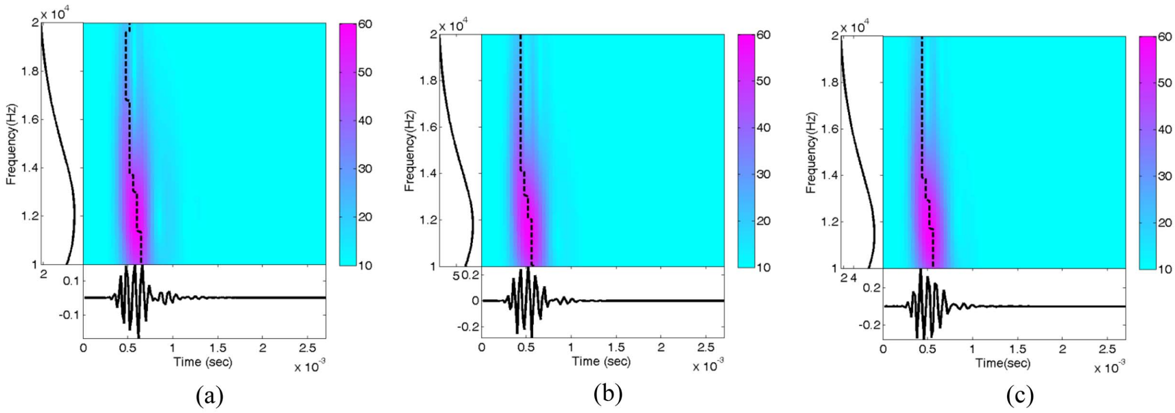

Fig. 15 SWFOMS for three linear predicted waveforms induced by the fourth impact: (a) sensor S_1, (b) sensor S_2 and (c) sensor S_3

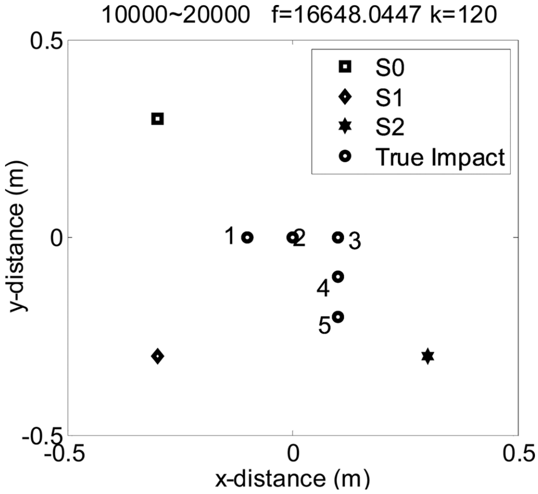

Fig. 16 Source localization for five impacts and comparison between true points and estimated points

frequency method was applied to the smoothed direct waves to obtain the arrival time difference. For example, Fig. 15 shows the results of time-frequency analysis for the first three smoothed direct waves due to the fourth impact. The SWFOMS time-frequency method was applied to these signals. In the figures, the horizontal axis presents time and the vertical axis presents frequency. The dashed lines in the center part in each map correspond to the peak amplitude. The arrival time difference for the waveform measured by the sensors was obtained from the time difference of the three dashed lines. The time differences due to other impacts were obtained in the same fashion as in the case of the fourth impact. The theoretical group velocity and phase velocity for the A_0 mode in a steel plate were obtained by reference to elastodynamics theory. The locations of impact loads were estimated by using triangulation. Fig. 16 shows the locations of the impact loads as estimated by triangulation based on the arrival time difference, which was obtained by using the SWFOMS for the pre-processed signal, and based on the theoretical group velocity. The circles in Fig. 16 indicate the true impact locations and the numbers indicate the serial impact locations estimated by the novel method proposed in this paper. There was some discrepancy between the true locations and the estimated locations. This error was caused by the theoretical group velocity and by some experimental error due to impact location and sensor position. The theoretical group velocity is not exact due to the properties of the tested material.

5. Conclusions

This paper presents a new approach for the source localization of multiple impacts in an isotropic plate structure. The proposed approach is based on a pre-processing method. The pre-processing method is to filter the measured waveform by using a band pass filter conditioned to select for low frequency f_L and a linear-prediction filter designed using Wiener-Horf optimization theory. Two major problems must be overcome to achieve source localization of serial multiple impacts: the overlapping of dispersive waves induced by multiple impacts and the reflection of those waves at the edge of the plate. The overlapping problem can be solved by adapting a band pass filter. The low frequency limit f_L is suggested for the band pass filter by reference to the relationship between impact interval Δ and the arrival time t_L of the dispersive waves at that low frequency f_L. The selection of the sensor to measure the Lamb wave in the plate should be carefully considered because of the high frequency limitation. If an accelerometer is selected, a high frequency limit is required because of its resonance frequency. In this study, a piezo-electronic displacement sensor was designed for the measurement of displacement without limitation at high frequencies. The reflection problem can be solved by chopping the filtered waveform to get only the direct wave and by smoothing the chopped wave through a linear-prediction filter in order to smooth the high frequency component at the chopped segment. The chopping time t_c is determined by using the time history of the simulated wave, which is numerically calculated. Details of the procedure for the source localization of multiple impacts are illustrated in this study by applying the proposed method to an isotropic steel plate. The method successfully localized the sources of five serial impacts.

Acknowledgements

This work was supported by grants from the National Research Foundation of Korea (NRF) funded by the Korean government (MEST) (No. 2009-0084728 and No. 2010-0014260).

References

Alleyne, D. and Cawley, P.A. (1991), “Two-dimensional Fourier transform method for the measurement of propagating multimode signals”, *J. Acoust. Soc. Am*., **89**(3), 1159-1168.

Balasubramaniam, K. and Rose, J.L. (1991), “Physically based dispersion curve feature analysis in the NDE of composites”, *Res. Nondestruct. Eval*., **3**(1), 41-67.

Cohen, L. (1995), *Time-Frequency Analysis* , Prentice hall, New Jersey.

Fonollosa, J.R. and Nikias, C.L. (1993), “Wigner-higher-order moment spectra definition, properties, computation and application to transient signal analysis”, IEEE Transactions on Signal Processing, **41**, 245-266.

Graff, K.F. (1953), *Wave Motion in Elastic Solids*, Dover Publications Inc., New York.

Haykin, S. (2007), *Adaptive Filter Theory* , Prentice hall, New Jersey.

Hellier, C.J. (2003), *Handbook of nondestructive evaluation* , McGraw-Hill company.

Lee, S.K. (1998), *Adaptive Signal Processing and Higher Order Time Frequency Analysis for Acoustic and Vibration Signatures in Condition Monitoring,* Ph.D. Thesis, University of Southampton.

Lee, S.K. and Whit, P.R. (2001), “Fault diagnosis of rotating machinery using wigner higher order moment spectra”, *Mech. Syst. Signal Pr*., **11**, 637-650.

Lee, S.K. Banerjee, S. and Mal, S. (2007), “Identification of impact force on a thick plate based on the elastodynamics and higher-order time-frequency analysis” *Proceedings of the Institution of Mechanical Engineers Part C-Journal of Mechanical Engineering Science*.

Lih, S.S. and Mal, A.K. (1995), “On the accuracy of approximate plate theories for wave field calculations in composite laminates”, *Wave Motion,* **21**(1), 17-24.

Loutridis, S. Douka, E. Hadjileontiadis, L.J. and Torchidis, A. (2005), “A two dimensional wavelet transform for detection of cracks in plates”, *Eng. Struct*., **27**(9), 1327-1338.

Mindlin, R.D. (1951), “Inluence of rotatory inertia and shear flexural motion of isotropic, elastic plate”, *J. Appl. Mech - T ASME*, **18**, 31-38.

Park, J.H. and Kim, Y.H. (2006), “Impact source localization on an elastic plate in a noisy environment”, *Meas. Sci. Technol*., **17**(10), 2757-2766.

Park, S.W. and Lee, S.K. (2010), “Development of a new sound metric for impact sound in a passenger car

using the wavelet transform", *Int. J. Autom. Technol.*, **11**, 809-818.
Pham, D.T., Ji, Z., Yang, M., Wang, Z. and Al-Kuthbi, M. (2007), "A novel human-computer interface based on passive acoustic localization", Human-Computer Interaction LNCS 4551 901-909.
Prosser, W.H. Seale, M.D. and Smith, B.T. (1999), "Time-frequency analysis of the dispersion of Lamb modes", *J. Acoust. Soc. Am*., **105**(5), 2669-2676.
Raghavan, A. and Cesnik, C.E.S. (2007), "Guided-wave signal processing using chirplet matching pursuits and mode correlation for structure health monitoring", *Smart Mater. Struct*., **16**(2), 355-366.
Rolshofen, W., Pham, D.T., Yang, M., Ji. Z. and Al-Kutubi, M. (2005), "New approach in computer interaction with tangible acoustic interface", *Proceedings of the IPROMs2005 Visual Conference*.
Tobis, A. (1976), "Acoustic Emission Source Location in two dimensions by an array of three sensors", *Non-Destructive Testing*, **9**(1), 9-12.
Ziola, S.M. and Gorman, M.R. (1991), "Source location in thin plates using cross-correlation", *J. Acoust. Soc. Am*., **90**, 2551-2556.

JK

Appendix A. Source localization with triangulation method

In order to locate the impact source at an arbitrary point on the surface of an isotropic plate, three sensors are placed on the same side on its surface and three intersecting circles are drawn, each centered at a sensor, with their radii determined by the travel times of the wave energy from the impact source to the respective sensor. By solving the three resulting simultaneous equations, a closed form expression for the source location can be obtained (Ziola and Gorman 1991, Tobis 1976). If the sensors are located at S_1 (0, 0, 0), S_2 (x_1, x_2, 0) and S_3 (x_1, x_2, 0), then the polar coordinates of the source point, (r, θ), are given by

$$r = \frac{A_2}{2(x_1 \cos\theta + x_2 \sin\theta + \delta_1)_{S_2}}, = \frac{A_3}{2(x_2 \cos\theta + x_2 \sin\theta + \delta_2)_{S_3}} \tag{7}$$

where $A_2 = S_2(x_1)^2 + S_3(x_1)^2 - \delta_1^2$ and $A_3 = S_2(x_2)^2 + S_3(x_2)^2 - \delta_2^2$, $\delta_1 = t_1 v_g$ and $\delta_2 = t_2 v_g$, v_g is the group velocity of the waves, and t_1 and t_2 are the time differences between sensors S_1-S_2 and S_1-S_3, respectively. The angle θ is obtained from the equation

$$\cos(\theta - \varphi) = K \tag{8}$$

where

$$K = [(A_3\delta_1 - A_2\delta_2)/B] \tag{9}$$

$$B = \left[\left(A_2 S_3(x_1) - A_3 S_1(x_1)\right)^2 + \left(A_2 S_3(x_2) - A_3 S_1(x_2)\right)^2 \right]^{1/2} \tag{10}$$

and

$$\tan\phi = \left[\left(A_2 S_3(x_2) - A_3 S_1(x_2)\right) / \left(A_2 S_3(x_1) - A_3 S_1(x_1)\right) \right] \tag{11}$$

Thus, the quantities to be extracted from the signals are the differences between the wave arrival times at the sensors. For the estimation of the radii of the circles, the group velocity of the waves is also required in addition to their arrival times.

Appendix B. Sliced Wigner fourth-order moment spectra (SWFOMS)

The general Wigner higher order moment spectra (WHOMS) of order n+1 for signal $x(t)$ is defined by Fonollosa and Nikias (1993) as

$$W_{n+1}(t, f_1, .., f_n) = \int_{\xi} X^*\left(\sum_{i=1}^{n} f_i + \frac{1}{n+1}\xi\right) \cdot \prod_{i=1}^{n} X^{(*)^{i+1}}\left(f_i - \frac{1}{n+1}\xi\right) e^{-j2\pi\xi t} d\xi \tag{12}$$

where n=1 and n=3 are the Wigner-Ville distribution (WVD) and the Wigner fourth order moment spectrum (WFOMS), respectively. Although the WHOMS has significant resolution advantages over other time-frequency methods, its application is obstructed by problems associated with cross/interference terms. In general, the $n+1^{\text{th}}$ order Wigner distribution for two-component signals is the sum of 2^{n+1} distributions, of which two are auto-terms and 2^{n+1}-2 are cross-terms. To reduce these cross-terms, it is common to consider a subset of the WHOMS called the principal slice. The principal slice is defined as the only plane in which a single complex exponential appears as a Dirac delta. This plane for the WFOMS is obtained by setting $f_1 = -f_2 = f_3 = f$ and $n = 3$ in Eq. (12). This is called the SWFOMS (sliced Wigner fourth order moment spectra). This slice generally includes both auto-terms and cross-terms, and the number of cross-terms is significantly reduced. The remained oscillating cross-terms are smoothed via conventional smoothing, which is processed by multiplying the ambiguity function of the SWFOMS by the kernel function. However, conventional smoothing fails to reduce the non-oscillating cross-terms (Lee and Whit 2001) since these non-oscillatory terms are difficult to distinguish from the auto-terms. In order to effectively smooth the non-oscillating cross-terms in the SWFOMS, consider the frequency version of the WVD

$$W(t,f) = \int_{\xi} X^*\left(f + \frac{1}{2}\xi\right) X\left(f - \frac{1}{2}\xi\right) e^{-j2\pi\xi t} d\xi \tag{13}$$

The pseudo Wigner distribution (PWD) (Cohen 1995) can be written by using the frequency domain windowing function $H(\xi/2)$ as follows

$$\begin{aligned} W_{pw}(t,f) &= \int_{\xi} H(-\frac{\xi}{2}) H^*(\frac{\xi}{2}) X^*\left(f + \frac{1}{2}\xi\right) X\left(f - \frac{1}{2}\xi\right) e^{-j2\pi\xi t} d\xi \\ &= \frac{1}{2}\int_{\xi'} H(-\xi') H^*(\xi') X^*(f+\xi') X(f-\xi') e^{-j2\pi\xi'(2t)} d\xi' \end{aligned} \tag{14}$$

where $\xi' = \xi/2$. Using convolution, Eq. (14) may be written as follows

$$W_{pw}(t,f) = X_h^*(f,2t) \underset{t}{*} X_h(f,2t) \tag{15}$$

where $X_h(f, t)$ is the short time Fourier transform (STFT) (Cohen 1995). Therefore, the PWD can be written as

$$\begin{aligned} W_{pw}(t,f) &= X_h^*(f,2t) \underset{t}{*} X_h(f,2t) \\ &= \int_{-\infty}^{\infty} X_h^*(f,t+\tau) X_h(f,t-\tau) d\tau \end{aligned} \tag{16}$$

In order to emphasize the auto-terms of the PWD for a multi-component signal, a window function $\gamma(\tau)$ can be incorporated into Eq. (16) and the smoothed Wigner distribution (SWD) can be developed as follows

$$W_{2,sw}(t,f) = \int_{-\infty}^{\infty} \gamma(\tau) X_h^*(f,t+\tau) X_h(f,t-\tau) d\tau \tag{17}$$

We refer to this window function as the γ method. In Eq. (17), when $\gamma(\tau)=1$, the SWD becomes the WVD, and when $\gamma(\tau)=\delta(\tau)$ the SWD becomes the spectrogram. Therefore, in order to smooth the cross-terms of the WVD for a multi-component signal, the duration T_γ for $\gamma(\tau)$ needs to be selected in accordance with

$$T_h < T_\gamma < \min_{i,j} \frac{t_i - t_j}{2} - T_h \tag{18}$$

where t_i and t_j are the temporal positions of the signal components and T_h is the duration of $h(t)$. The

SWD is obtained by convolving two signals $X_h(f, 2t)$ and $X_h^*(f, 2t)$ with respect to time and using the γ- method for smoothing the cross-terms in Eq. (17). Similarly, a smoothed version of the SWFOMS can also be obtained by the convolution of the two SWDs $W_{2,sw}(f, 2t)$ and $W_{2,sw}^*(f, 2t)$ with respect to time as follows

$$SWFOMS(t,f) = \frac{1}{2}\int_{\tau}\gamma(\tau)W_{2,sw}\left(f,t+\tau\right)\cdot W_{2,sw}^{*}\left(f,t-\tau\right)\,d\tau \tag{19}$$

Appendix C. Linear-prediction filter

The linear predictor filter consists of a linear transversal filter M with tap weight $f_1, f_2, \ldots, f_M$ and tap input $x(n\text{-}1)$, $x(n\text{-}2)$,., $x(n\text{-}M)$. We assume that these tap inputs are drawn from a wide sense stationary stochastic process of zero mean. The predicted value $\underline{x}(n)$ is obtained by

$$\underline{x}(n) = \sum_{n=1}^{M} f(k)x(n-k) \tag{20}$$

The prediction error $e(n)$ equals the difference between the input sample $x(n)$ and its predicted value $\underline{x}(n)$. Therefore, the minimum mean-squared prediction error is given by the cost function J,

$$J = E[|e(n)|^2] \tag{21}$$

Let $\boldsymbol{f}$ denote the M by 1 optimum tap-weight vector of the forward predictor. It is can be written in expanded form as

$$\boldsymbol{f} = [f_1, f_2, \ldots, f_M] \tag{22}$$

To solve the Wiener-Horf equation (Haykin 2007) for the vector $\boldsymbol{f}$, we require the knowledge of two quantities: (1) the M by M correlation matrix of the tap inputs $x(n\text{-}1)$, $x(n\text{-}2)$,…., $x(n\text{-}M)$, and (2) the M by 1 cross-correlation vector between these inputs and the desired response $x(n)$. To evaluate J, a third quantity is required, the valiance of $x(n)$. We now consider these three quantities, one by one:

1. The tap inputs $x(n\text{-}1)$, $x(n\text{-}2)$,…., $x(n\text{-}M)$ define the M by 1 tap input vector, $\boldsymbol{x}(n\text{-}1)$, as shown by

$$\boldsymbol{x}(n-1) = [x(n-1), x(n-2), \ldots, x(n-M)]^T \tag{23}$$

Hence, the correlation matrix of the tap inputs equals

$$\begin{aligned}\boldsymbol{R} &= E[\boldsymbol{x}(n-1)\boldsymbol{x}^T(n-1)] \\ &= \begin{bmatrix} r(0) & r(1) & \cdots & r(M-1) \\ r(1) & r(0) & \cdots & r(M-2) \\ \vdots & \vdots & \ddots & \vdots \\ r(M-1) & r(M-2) & \cdots & r(0) \end{bmatrix}\end{aligned} \tag{24}$$

where $r(k)$ is the auto-correlation function of the input process for lag k, where $k = 0, 1, \ldots, M\text{-}1$,

2. The cross correlation vector between the tap input $x(n\text{-}1)$, ..., $x(n\text{-}M)$ and the desired response $x(n)$ equals

$$\mathbf{g} = E\left[\mathbf{x}(n-1)x(n)\right] = \begin{bmatrix} r(1) \\ r(2) \\ \vdots \\ r(M) \end{bmatrix} \tag{25}$$

3. The variance of $x(n)$ is equals to $r(0)$, since $x(n)$ has zero mean.

By using these three quantities, the Wiener-Hopf equation to solve the forward linear prediction problem is obtained and given by

$$\boldsymbol{f} = \boldsymbol{R}^{-1}\boldsymbol{g} \tag{26}$$